JOURNAL OF CATALYSIS 39, 265–276 (1975)

On the Mechanism and Kinetics of the CO-Oxidation Reaction on Polycrystalline Palladium

I. The Reaction Paths[1]

T. MATSUSHIMA AND J. M. WHITE

Department of Chemistry, University of Texas, Austin, Texas 78712

Received February 19, 1975

Transient phenomena, which occur in the oxidation reaction of carbon monoxide catalyzed by palladium, have been characterized. The substrate, a polycrystalline palladium foil initially exposed to relatively large amounts of oxygen at high temperatures, was dosed alternately with oxygen and carbon monoxide and transient carbon dioxide production was monitored mass spectrometrically. Two different reaction paths were found to prevail. When oxygen is preadsorbed, exposure to carbon monoxide leads to carbon dioxide through $CO(g) + O(a) \rightarrow CO_2(g)$, an Eley–Rideal path. When the dosing sequence is reversed, a Langmuir–Hinshelwood reaction occurs, $CO(a) + O(a) \rightarrow CO_2(g)$. The former reaction can be used to quantitatively titrate surface oxygen and two methods of analysis can be used to determine the amount of adsorbed oxygen under working conditions. One method is useful when the working pressure of CO is low while the other is useful when it is high.

INTRODUCTION

Numerous investigations have been reported in the literature on the oxidation of CO on the transition metals Pd and Pt (*1–18*). Studies of this reaction at relatively low pressures, 10^{-4}–10^{-6} Pa, by Ertl and co-workers (*12–16*) have shown that different kinetic behavior obtains below and above 473 K with the adsorption–desorption characteristics of CO controlling the kinetic features. Carbon monoxide begins desorbing at about 373 K and is nearly completely desorbed at about 473 K. The main features of the reaction are characterizable at all temperatures by an Eley–Rideal mechanism involving adsorbed oxygen atoms and gas phase CO. These observations hold for Pd(100) (*15*), Pd(110) (*12*), Pd(111) (*14*), and polycrystalline Pd wire (*15*). There does appear to be an additional contribution from a Langmuir–Hinshelwood mechanism involving adsorbed oxygen atoms and adsorbed CO (*16*). On polycrystalline palladium ribbons, exposed to relatively large amounts of oxygen at high temperatures near 900 K and for which there is evidence of considerable oxygen uptake by the substrate, Close and White (*17*) found three distinct rate laws depending on the temperature for the case $CO/O_2 \geq 1$. Using substrates prepared in the same way Matsushima *et al.* (*18*) have explored in considerable detail the kinetic features of the above temperature regions, $T < 473$ K, $473\ \text{K} < T < 700$ K, and $T > 700$ K, for pressures in the range 10^{-3}–10^{-7} Pa and $0.1 \leq CO/O_2 \leq 20.0$.

In order to rationalize the complex features of the overall reaction, it is helpful to have kinetic data for the constituent processes as well as data for the overall reaction. Data measuring the amount of adsorbed species, especially under working conditions (*19*), is also very useful. In this paper our aims have been to establish a method for evaluating the amount of

[1] Supported in part by the National Science Foundation Grant GP-37974.

adsorbed oxygen on the substrate in the course of the reaction, to elucidate the possible reaction paths, and to determine the kinetics of some of the steps in the mechanism. These goals were approached using a titration method similar to that employed by Bonzel and Ku (*9*) in their study of CO-oxidation over Pt and using analysis of CO_2 decay curves following oxygen dosing under various conditions. We also present here detailed data for oxygen adsorption.

II. EXPERIMENTAL METHODS

Some aspects of the apparatus and experimental procedure have been reported previously (*17*). The system was a bakeable ultrahigh vacuum apparatus in which pressures were monitored with a Bayard-Alpert gauge and a quadrupole mass spectrometer. Since our experiments were carried out in the range 10^{-4}–10^{-6} Pa, we used the vacuum system in a routine fashion such that the base pressures achieved were less than 5×10^{-7} Pa, the principal residual being CO. During experiments the system was continuously pumped by an ion pump.

The substrate was a rectangular shaped piece of polycrystalline Pd foil ($20 \times 5 \times 0.13$ mm). Prior to the oxidation experiments it was exposed to oxygen at a pressure of 10^{-4} Pa and a temperature of 900 K. This treatment has been shown to be sufficient for the establishment of stable catalyst behavior (*17*). During a series of measurements the oxygen-exposed substrate was heated to 900 K for about 5 min prior to each experiment. The substrate temperature was monitored with an iron–constantan thermocouple spot-welded to the palladium foil. The foil itself was mounted on Pyrex-covered tungsten rods.

Reactant gases, CO and O_2, were introduced through independent continuously variable leak valves.

III. RESULTS AND DISCUSSION

1. Observed Transient Phenomena and Possible Reaction Paths

A typical experiment is outlined in Fig. 1 and is comprised of several segments involving dosing with CO or O_2 for various lengths of time and observation of CO_2 production during certain periods. Beginning under base vacuum at the left side of Fig. 1 with the catalyst at 573 K, a dose of

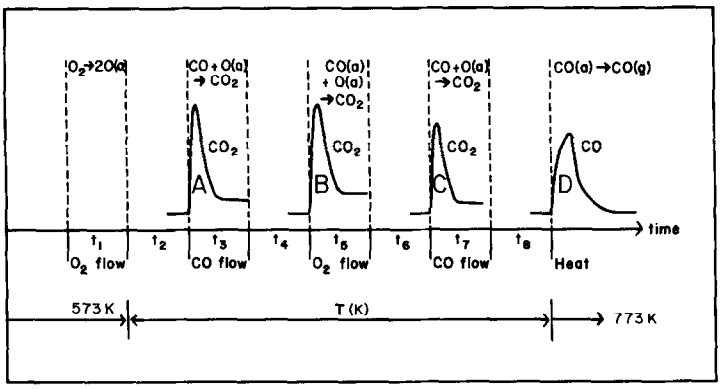

FIG. 1. Schematic description of the dosing and monitoring sequence of a typical experiment. The temperature is varied in three discrete steps. There are two oxygen doses, one at 573 K for time t_1 and the other at temperature T for time t_5. Carbon monoxide is applied in two doses, both at temperature T and during periods t_3 and t_7. During oxygen or carbon monoxide dosing none of the other reagent is being added. No reactant is added during the periods t_2, t_4, t_6, t_8 and t_9. Following t_8 the system is flashed to 773 K. Peaks A, B, and C represent the transient CO_2 production occurring during the time intervals in which they occur. Peak D represents desorbed CO.

oxygen at a fixed pressure of 1.3×10^{-5} Pa was applied for a time t_1. The oxygen dose was then terminated and the substrate temperature reduced to T and held there under vacuum for a period t_2. While monitoring CO_2 at $m/e = 44$, peak A, the substrate was dosed for a time t_3 with CO. The CO dose was terminated and the pressure was reduced for the period t_4 after which, the substrate, still at temperature T, was exposed again to oxygen for a time t_5. During this interval CO_2 production was monitored, peak B. This was followed by closing the oxygen leak, evacuating for a period t_6, and exposing to CO for a period t_7 during which time peak C was noted. After evacuating for a time t_8, the substrate was flashed to 773 K and the CO desorption at $m/e = 28$ was monitored. Obviously we are interested in using the features of the four peaks A, B, C, and D as a means of characterizing the system. These are considered in detail below.

Peak A. This peak was studied following an oxygen dose of 3.6×10^{-3} Pa · s (oxygen pressure multiplied by exposure time) at 573 K and Fig. 2 shows peak A for a variety of conditions as outlined in the legend. Period t_2 varied depending on the temperature with longer evacuation periods required at lower temperatures in order to reach the desired temperature. The range of t_2 was 180 s at 573 K to 540 s at 300 K, and the dosing period t_3 was 120 s. As noted in the Fig. 2 legend, the CO dosing pressure varied from 7.18×10^{-5} Pa at 573 K to 2.66×10^{-4} Pa at 300 K. The areas under the various peaks were calculated using the CO_2 pressure after about 120 s as a base line. This base line is shown as the horizontal broken line for peak 1 in Fig. 2. Examining the curves of Fig. 2, we note some dependence of peak height and width on experimental conditions. In spite of the variable nature of T, t_2, and p_{CO}, the areas under the peaks in Fig. 2 are constant within ±20%. Another important feature of the CO_2 pressure profiles is their rapid onset following exposure to CO. There is no detectable time lag for the production of CO_2 and no detectable change in the slope of the onset portion of the CO_2 versus time curves as the experimental conditions, es-

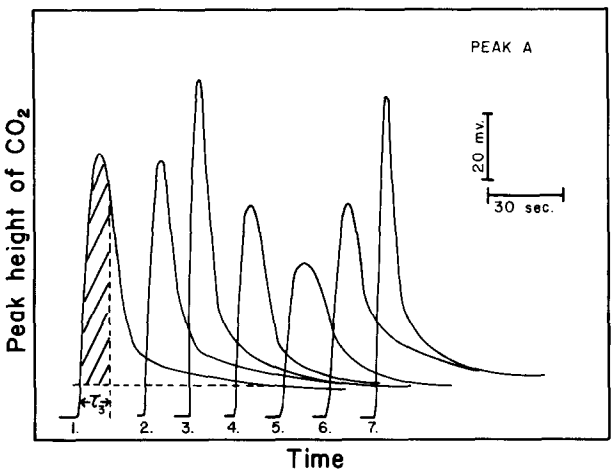

FIG. 2. Characteristics of peak A under various experimental conditions. Oxygen dose = 3.6×10^{-3} Pa · s at 573 K. Peaks are shifted with respect to each other for easier viewing. CO dose began at the sharp break in each curve. The broken horizontal line encloses that portion of the peak used in the area determinations while the cross-hatched area is 63% of the total peak area and is used to define a reaction lifetime τ_3 (see Table 1). The data for each of the peaks in the form $\{t_2, T, p_{CO}\}$ is: (1) 180 s, 573 K, 7.18×10^{-5} Pa; (2) 180 s, 473 K, 7.58×10^{-5} Pa; (3) 180 s, 441 K, 1.17×10^{-4} Pa; (4) 180 s, 393 K, 9.31×10^{-5} Pa; (5) 240 s, 353 K, 7.98×10^{-5} Pa; (6) 300 s, 318 K, 1.33×10^{-4} Pa; (7) 540 s, 300 K, 2.66×10^{-4} Pa.

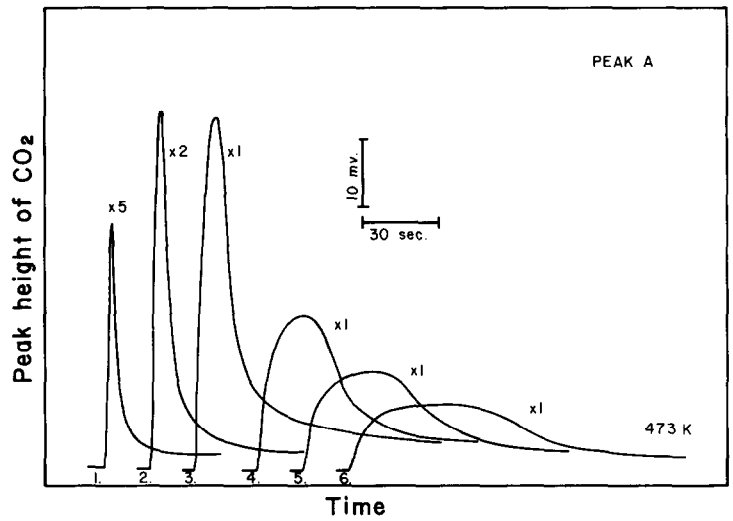

FIG. 3. Variation of peak A with CO dosing pressure. O_2 dose = 1.15×10^{-3} Pa · s at 473 K, t_2 = 60 s, CO background during O_2 dosing = 4.0×10^{-7} Pa, CO_2 background = 8.0×10^{-7} Pa. Final CO dosing pressures for the individual peaks are: (1) 3.05×10^{-4} Pa; (2) 1.25×10^{-4} Pa; (3) 4.92×10^{-5} Pa; (4) 2.00×10^{-5} Pa; (5) 1.46×10^{-5} Pa; (6) 1.02×10^{-5} Pa.

pecially temperature, are varied as described in Fig. 2.

There is, however, an important change in the height and width of peak A which can be characterized by working at constant O_2 dose, constant T, and constant t_2. Figure 3 and Table 1 summarize our observations at O_2 dose = 1.15×10^{-3} Pa · s, $T = 473$ K, and $t_2 = 60$ s. During the O_2 dosing period the background CO and CO_2 pressures were typically 4.0×10^{-7} and 8.0×10^{-7} Pa, respectively. As the CO dosing pressure is varied from 1.02×10^{-5} to 3.06×10^{-4} Pa the height of peak A follows proportionally. As shown in the fourth column of Table 1 the peak area shows no dependence on the CO dosing pressure until it is reduced to below 4.0×10^{-5} Pa. Below this pressure there is considerable opportunity for making a significant error in computing the peak areas due to the very broad peaks which become difficult to distinguish from the CO_2 background. The CO pressures given in Table 1 are those measured just after the CO_2 peak A has occurred. Our data are reminiscent of those on Pt (9).

TABLE 1
KINETIC DATA FOR PEAK A

p_{CO} (10^{-5} Pa)	Lifetime, τ_3 (s)	Collision number of CO during τ_3 (10^{15} collisions cm^{-2})	Relative area of peak A
30.5[a]	3.6	3.5[b]	1.0
12.5	6.2	2.4	0.97
8.51	7.2	1.9	1.0[c]
8.91	7.2	2.0	1.0
6.78	9.6	2.1	1.0
5.32	12.0	2.0	1.0
4.92	12.0	1.9	1.0
2.00	25.0	1.6	0.87
1.66	29.0	1.5	0.76
1.46	35.0	1.6	0.85
1.02	49.0	1.6	0.77

[a] See caption of Fig. 3 for other experimental conditions.

[b] 1 Langmuir of CO = 4.2×10^{14} collisions cm^{-2} at 300 K.

[c] Standard.

Using the first 63% of the peak area as a criterion for a reaction time, we can compare collision numbers during this time τ_3. The time τ_3 is illustrated in Fig. 2 for the first peak. The collision number during τ_3 is calculated on the basis of a 300 K Boltzmann distribution. Columns 2 and 3 of

Table 1 summarize τ_3 and the collision numbers. Since the collision numbers are calculated on the basis of the final CO pressure, the values in Table 1 are too large by about 30–40%. This occurs because, during the time that CO_2 is being produced, the CO pressure is lower than its final steady-state value. Comparing lifetimes and the collision numbers we see that while the lifetime varies by a factor of 10 the collision number varies, at most by a factor of 2. The actual variation in the latter quantity is probably less since for short lifetimes the response of our instrumentation will lead to an overestimate of τ_3. On this basis we conclude that there is at most a very weak dependence of the collision number on CO pressure. This implies that the production of CO_2 in peak A is first order with respect to CO pressure, p_{CO}.

During t_1 and t_2, the surface is considered to be covered by oxygen while during t_2 and t_3 the ambient O_2 pressure is negligibly small and furthermore adsorbed oxygen is not desorbed at these temperatures (*17*). Therefore, oxygen which participates in CO_2 formation must come from adsorbed species on the surface. We have to consider two possibilities, as follows:

$$CO(g) + O(a) \rightarrow CO_2(g), \qquad (1)$$

$$CO(a) + O(a) \rightarrow CO_2(g), \qquad (2)$$

where O(a) is an adsorbed oxygen atom. However process (2) has a different kinetic behavior from peak A, as discussed below. This observation and the data of Figs. 1–2 and Table 1 suggest that the CO_2 production described by peak A arises primarily from an Eley–Rideal process, $CO(g) + O(a) \rightarrow CO_2(g)$, and the area of peak A measures the amount of adsorbed oxygen available for CO oxidation. As discussed below the areas of the curves in Fig. 3 correspond to O(a) amounts near saturation. The collision numbers given in Table 1 therefore indicate that a large percentage of the collisions lead to CO_2. This is consistent with the data of Fig. 2 which can be analyzed for collision numbers corresponding to the lifetime τ_3. A logarithmic plot of the collision numbers versus T^{-1} indicates a very small activation energy of 5.9 kJ mol^{-1}.

Peak B. As illustrated in Fig. 1, peak B occurred after the substrate was dosed with both oxygen (t_1) and carbon monoxide (t_3). During period t_3 oxygen was used up and at the end of this period surface oxygen available for making carbon dioxide was nearly exhausted. Thus, in the latter stages of t_3 the substrate was exposed to CO under conditions of very low oxygen coverage. With both the CO and O_2 valves closed, the system was evacuated for a period t_4 typically 180 to 480 s. During all this time the substrate was maintained at temperature T. Following t_4, dosing with oxygen for a period t_5 furnished another transient of CO_2 production, peak B.

Figure 4 shows that peak B has an area and shape which are very sensitive to the temperature T. Below 325 K (peaks 7 and 8) adding CO gives a slight increase in the background level at $m/e = 44$ but nothing attributable to the transient production of CO_2 at the substrate surface. Between 338 and 393 K and CO_2 production rate shows two maxima. These peaks are characterized by much slower rise-times and much longer decay times than peak A. Above 440 K the peak sharpens, decreases in area and eventually disappears altogether near 473 K.

Since the background CO pressure at the beginning of period 5 was very low, the transient CO_2 production cannot be due to residual gas phase CO which was in the system following period t_4. Rather, the CO_2 observed during t_5 must be related to adsorbed CO present at the beginning of this period. The reaction time τ_5, defined in the same way as for peak A, is almost the same as for peak A when $T = 393$ K. As

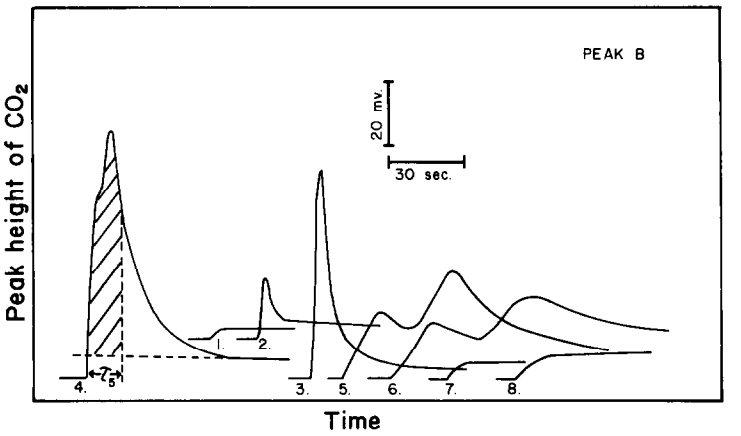

FIG. 4. Temperature dependence of peak B. Dose period t_5 = 120 s. Data for the peaks in the form $\{t_4, T, p_{O_2}\}$ are as follows: (1) 180 s, 573 K, 5.32×10^{-5} Pa; (2) 180 s, 473 K, 5.05×10^{-5} Pa; (3) 180 s, 441 K, 3.72×10^{-5} Pa; (4) 180 s, 393 K, 6.12×10^{-5} Pa; (5) 180 s, 351 K, 6.38×10^{-5} Pa; (6) 480 s, 338 K, 1.33×10^{-4} Pa; (7) 180 s, 317 K, 1.73×10^{-4} Pa; (8) 300 s, 300 K, 3.19×10^{-4} Pa.

the temperature decreases below 393 K the reaction time shows a marked increase in contrast with peak A. On this basis we conclude that some activation energy is required for the reaction producing peak B.

Three candidate reaction paths for peak B are examined here.

$$
\begin{aligned}
(1)\quad & CO(a) \rightarrow CO(g),\\
& \tfrac{1}{2}O_2(g) \rightarrow O(a),\\
& CO(g) + O(a) \rightarrow CO_2(g),\\
(2)\quad & CO(a) + O_2 \rightarrow CO_2(g) + O(a),\\
(3)\quad & CO(a) \rightarrow CO(g),\\
& \tfrac{1}{2}O_2(g) \rightarrow O(a),\\
& CO(a) + O(a) \rightarrow CO_2(g).
\end{aligned}
$$

Path (1) requires the desorption of CO and asserts that an Eley–Rideal mechanism is operative in which the desorbed CO collides with O(a) on the substrate surface to form CO_2. At T = 393, 350 and 338 K the areas are very nearly the same as those for the corresponding temperature in Figs. 2 and 3 (peak A). Since the system is pumped continuously and the only source of CO is the substrate surface there is no way this path can contribute significantly to the observed CO_2 because insufficient gas phase CO is available.

Reaction path (2), if the major contributor, should always show the largest rate at the onset of the O_2 dosing period regardless of the temperature since the amount of CO(a) is largest at this time. Referring to Fig. 4 and comparing peaks 3–6 this is clearly not always the case. The rise-times of peaks 4–6 are clearly different and are significantly longer than the response time of our system (compare with the rise-times of Figs. 2–3). We thus conclude that path 2 is not the major contributor to peak B although above 393 K it can not be definitely ruled out if a change in reaction path occurs as the temperature varies.

The candidate of choice is path (3) which is a Langmuir–Hinshelwood process involving adsorbed CO and O. This process, like path (1), involves the chemisorption of oxygen and the desorption of carbon monoxide. The distinction between the two is that reaction between adsorbed CO and O occurs in path (3) but does not in path (1). To account for the experimental observations using path (3) requires that, at low temperatures, we regard the CO desorption step as slow compared to the reaction between CO(a) and O(a).

Using path (3) as a model, the temperature dependence of the characteristics of

peak B can be accounted for as follows: At low temperatures, the CO coverage at the beginning of period 5 is large and can not be replaced by oxygen. Thus, any reaction involving O(a) cannot occur. Any potential reaction between gas phase O_2 and adsorbed CO to produce CO_2 is so slow that the CO_2 production above background cannot be detected. This holds for temperatures up to about 320 K. As the temperature is increased to 338 K, curve 6 of Fig. 4, the rate of CO_2 production increases and a double-peaked curve appears which persists to temperatures up to 393 K. The rise-time of these curves is obviously much longer than for peak A curves at the same temperature. There must, therefore, be some difference in the reaction paths for peaks A and B. Comparing curves 4–6 of Fig. 4 a clear trend emerges toward shorter rise-times and shorter reaction times. In this intermediate temperature interval, 338 to 393 K, a small amount of CO desorption occurs during the evacuation interval t_4. Thus when the O_2 dose is applied, adsorption of oxygen can occur. This adsorption is limited by the CO coverage retained after t_4. Reaction between O(a) and CO(a) then occurs with some activation energy; thus both the reaction time and the rise-time decrease with increasing temperature. The rise-time is also related to the CO surface coverage at the beginning of period t_5 but only weakly. Between 338 and 393 K this initial coverage decreases slightly and therefore allows slightly larger oxygen coverage to be attained in the early stages of period 5. Consequently, the rise-time decreases slightly. Thus our model, CO(a) + O(a), is supported by the peak shape which shows a temperature dependent maximum occurring sometime after the beginning of the O_2 dose. The double-maximum character of the CO_2 production curves in this temperature range may be due to two kinds of CO(a). This problem is being investigated further.

Between 393 and 573 K the rise-time remains short while the peak area rapidly diminishes to zero. In this region, the desorption rate of CO increases rapidly with temperature as indicated by peak D, which is discussed below, and by earlier flash desorption measurements under these conditions (*17*). Thus during the evacuation period t_4 the coverage of carbon monoxide is reduced readily and, while oxygen adsorption occurs rapidly and becomes large at the beginning of period t_5, there is little CO left with which it can react to form CO_2. Approaching 573 K the CO coverage is nearly zero and as a result the CO_2 produced is also nearly zero.

In the above paragraphs our qualitative description of peak B has been in terms of a Langmuir–Hinshelwood reaction between CO(a) and O(a). The quantitative determination of CO(a) from an analysis of peak B is possible except at higher temperatures where desorption of CO occurs and CO(a) becomes very small (*9,16,20*).

Assuming the reaction between CO(a) and O(a) is rate controlling for peak B, it is possible to estimate an activation energy for the process by plotting the logarithm of the maxima of the CO_2 production rates versus T^{-1}. Since the maxima should appear when CO(a) = O(a), they should be proportional to the rate coefficient of the reaction (*16*). Referring to Fig. 4 and using the second peak in the double-peaked curves, since it always predominates, such a plot furnishes an estimated activation energy of 19.4 kJ mol^{-1} (*20*).

Peak C. The conditions surrounding period 7 are much like those of period 3 except the CO dose is applied to a substrate having a recent history of O_2 and CO exposure at temperature $T < 573$ K. Above 323 K this is not particularly important since the previous CO has reacted during t_5 and the surface is covered with adsorbed oxygen at the beginning of period 7. Thus above 323 K peak C is essentially the same as peak A. Below 323 K, CO re-

tained from period 5 still covers the surface and an additional CO gives no CO_2 other than a slight increase in the background. The evacuation period t_6 was typically 180 s.

Peak D. This peak is a CO flash desorption spectrum of a substrate dosed with CO at temperature T. The shape of this peak is equivalent to that reported earlier by Close and White (*17*). At temperatures below 323 K the area is almost equal to the maximum value of the area of Peak A indicating that the maximum CO and O coverages are approximately equal under our experimental conditions. The point is discussed further below. Above 323 K the area of the CO desorption peak decreases rapidly with increasing T and above 443 K it becomes vanishingly small.

To sum up this section we note that it should be possible to determine the amount of adsorbed oxygen, which is available for CO oxidation, under working conditions using the titration method outlined above. The situation for carbon monoxide is more complicated since it desorbs as the temperature is raised through the interval 300–500 K. In those experiments involving CO dosage of an O_2 treated substrate an Eley–Rideal process predominates. When the exposure sequence is reversed a Langmuir–Hinshelwood process occurs. Peaks A, B, C and D show that the rate of the replacement of CO(a) by O(a) is very slow below 323 K, but increases rapidly with temperature. In the following sections we outline procedures for establishing quantitatively the amount of adsorbed oxygen under working conditions of the substrate.

2. *Transients Observed when a Steady-State CO–Substrate System is Dosed with Oxygen*

As a preliminary to the quantitative analysis procedure we carried out a different kind of dosing experiment in which a steady-state flowing CO–substrate system was established at 473 K and then dosed with a relatively large pressure of oxygen. Figure 5 depicts a typical case in which the initial CO pressure was 2.39×10^{-6} Pa, the O_2 dose pressure was 5.85×10^{-6} Pa, and the dose was for 300 s. On admission of O_2, the CO pressure dropped to 9.18×10^{-7} Pa while the

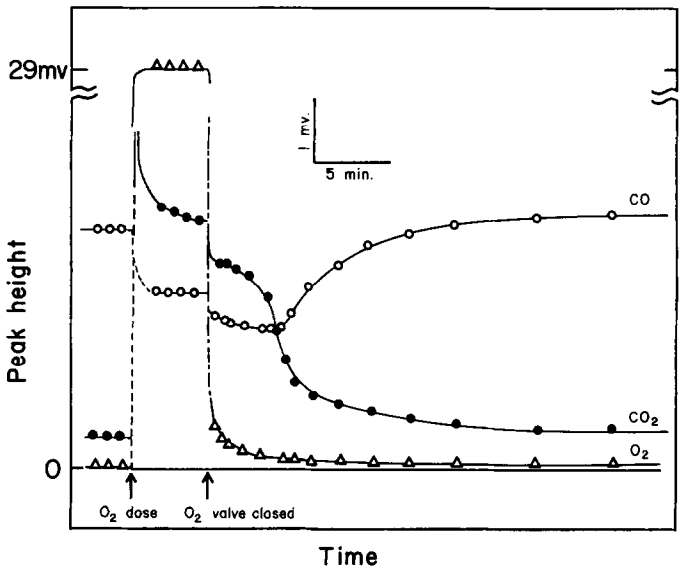

FIG. 5. Variation of CO, O_2, and CO_2 partial pressures before, during, and after oxygen dosing at 473 K. CO pressure prior to dosing = 2.4×10^{-6} Pa. O_2 dose = 5.9×10^{-6} Pa for 300 s.

CO_2 passed through a peak in the early stages of the dose after which it slowly stabilized. This sharp peak is attributed to the reaction between CO(a) and O(a), the Langmuir–Hinshelwood reaction, which is thus very fast at this temperature. After a short period the CO_2 production rate declines because the surface coverage of CO cannot be maintained in the presence of oxygen under these conditions. As described below, the reaction between adsorbed oxygen and gas phase CO becomes important under these conditions.

When the O_2 flow was stopped after 300 s, the O_2 partial pressure dropped very rapidly while changes in the CO and CO_2 partial pressures occurred with much longer time constants as shown in Fig. 5. Production of CO_2 during this period of low oxygen pressure is attributable to the Eley–Rideal reaction, $CO(g) + O(a) \rightarrow CO_2(g)$. The data of Fig. 5 clearly show that there is a significant adjustment of the surface coverage of CO when oxygen is admitted to the system and, at 473 K, oxygen coverage increases while carbon monoxide coverage decreases when the system is dosed as described above. It appears that in the late stages of the oxygen dose the reaction rate is controlled for the most part by the Eley–Rideal mechanism.

Referring again to peak A of Fig. 1, we found, as described in Sect. III, 3, that the area of this peak declined significantly as the evacuation period t_2 increased. This decay is interpreted, on the basis of the data of Fig. 5, as due to the reaction between adsorbed oxygen and the residual gas phase carbon monoxide in the system.

3. *Using Peak Areas as a Means of Analyzing the Amount of Adsorbed Oxygen*

For a fixed O_2 dosing pressure, the area of peak A depends on the oxygen exposure time t_1 and the evacuation interval t_2. In order to characterize the oxygen amount under the oxygen dosing conditions (i.e., working conditions for which $t_2 = 0$) a suitable extrapolation procedure is needed. For this purpose we have studied the dependence of the area of peak A on t_2. If the interpretation given in Sect. III, 2 is correct, then the area of peak A should decrease exponentially with t_2 since the reaction is $CO(g) + O(a) \rightarrow CO_2(g)$ and the integrated rate curve measures the amount of oxygen adsorbed at the beginning of period 3. Letting $Q(O)$ represent the amount of adsorbed oxygen atoms as measured by the area of peak A, we would then expect ln $Q(O)$ to decrease linearly with t_2. Figure 6 summarizes our experimental data in this form for $T = 473$ K and confirms this linear relation. Line 1 of Fig. 6 represents the case where an O_2 dose

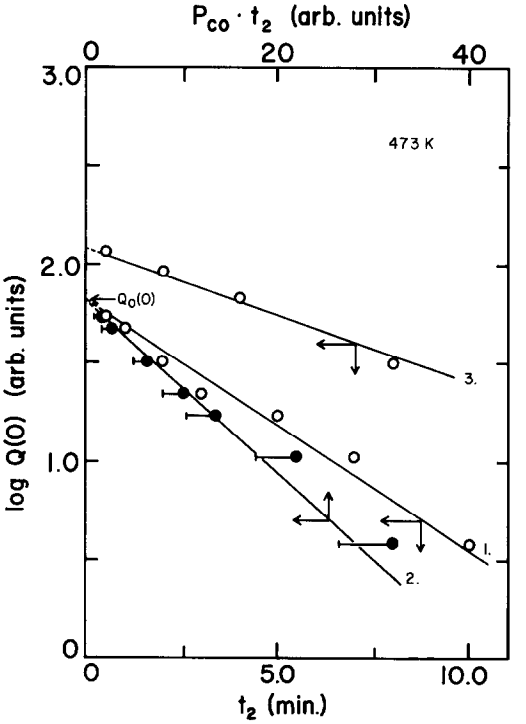

FIG. 6. Variation of amount of surface oxygen as determined by the area of peak A, with t_2 and $p_{CO}\, t_2$ at 473 K. (1) and (2) O_2 dose of 3.19×10^{-4} Pa · s; (3) dose of 9.57×10^{-4} Pa · s; (1) and (3) are plotted versus t_2 and (2) is plotted versus $p_{CO}\, t_2$ where p_{CO} is the carbon monoxide pressure measured prior to the O_2 dose and is about 1.3×10^{-6} Pa. The error bars on the enclosed points indicate the uncertainty of p_{CO}.

of 3.19×10^{-4} Pa · s (5.32×10^{-5} Pa for 60 s) was applied while line 3 is for a threefold higher dose achieved by increasing the dose time to 180 s.

The CO background pressure during t_2 was constant for a single experiment but showed small variations between experiments. As a result a more reliable way to make the extrapolation is to plot ln Q(O) versus $p_{CO}t_2$ where p_{CO} is the CO background pressure measured just prior to the oxygen dose at t_1. Line 2 of Fig. 6 shows a plot of this dependence for the data of line 1. The pressure of CO prior to t_1 is used because the dosing time is not long enough to accurately determine a background CO pressure and the CO pressure varies during t_2.

The desired coverage at $t_2 = 0$, Q_0(O), is determined by extrapolation of the curves of Fig. 6 to t_2 or $p_{CO} \cdot t_2 = 0$. As shown in Fig. 5, p_{CO} is nearly constant for a short period after the O_2 dose is completed but then it begins to rise. Referring to Fig. 1, this means that p_{CO} will show a tendency to rise during t_2, especially if it is large. Thus the slope of ln Q(O) versus t_2 will tend to increase as t_2 increases. For the conditions of Fig. 5 p_{CO} is nearly constant for about 300 s following the O_2 dose.

Some dependence of Q_0(O) on O_2 dose is indicated in Fig. 6 with about a twofold increase in the initial coverage arising when the dose is increased threefold from 3.2×10^{-4} to 6.4×10^{-4} Pa · s. Increasing the dose to 3.2×10^{-3} Pa · s gave no further increase in Q_0(O). Therefore the extrapolated value of 120 shown in Fig. 6 for line 3 is very close to the steady-state value for the conditions given. Since the maximum area of the CO desorption profile (peak D) determined in these same units is about 150, this oxygen coverage must correspond to saturation. The steady-state value is very nearly independent of p_{O_2} above 1.4×10^{-6} Pa.

4. *Determination of Oxygen Coverage by Analyzing the Decay of CO_2 After Oxygen Dosing*

Figure 5 shows a pronounced time lag in the decay of the CO_2 partial pressure. The

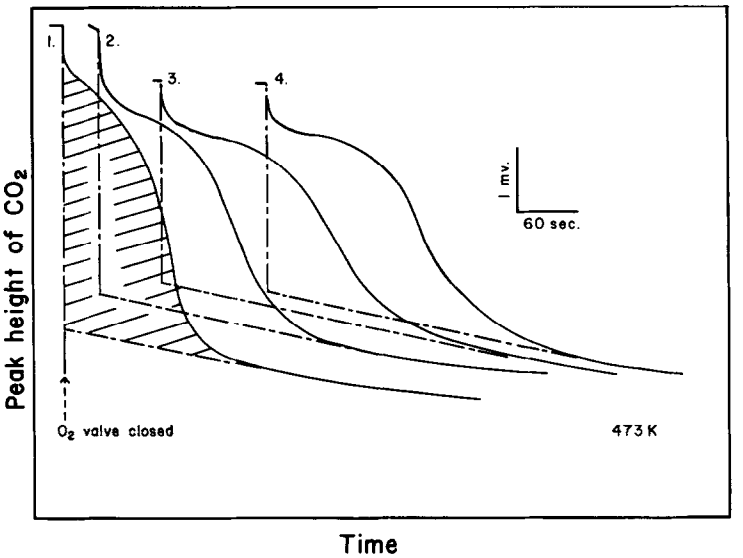

FIG. 7. Variation of CO_2 pressure decay with O_2 dose at 473 K. Initial value of $p_{CO} = 4.0 \times 10^{-6}$ Pa. O_2 dose pressure = 8.0×10^{-6} Pa. The oxygen dose and exposure time for each curve are: (1) 3.6×10^{-4} Pa · s, 45 s; (2) 7.2×10^{-4} Pa · s, 90 s; (3) 1.9×10^{-3} Pa · s, 240 s; (4) 3.4×10^{-3} Pa · s, 420 s. Note: The carbon monoxide pressure during the steady-state portion of the dose period was about 1.3×10^{-6} Pa.

time required for the decay increased as the O_2 dosing period increased. The background CO_2 pressure, reached several minutes after the termination of the oxygen dose, also increased with O_2 dosing period. Figure 7 shows how the CO_2 decayed with time following an O_2 dose at 473 K when the CO pressure prior to the O_2 dose was 4.0×10^{-6} Pa. These pressure–time profiles are characterized by an initial slowly declining pressure followed by a rapid drop to a background level which slowly decays. Since the background level increased with O_2 dose, it was extrapolated separately for each peak, as shown in Fig. 7, in order to provide a systematic way of estimating the amount of CO_2 produced after the oxygen dosing period. This area is shaded in Fig. 7 for curve 1. When the dose was less than 7.2×10^{-4} Pa · s the area showed some dependence on dosage but no dependence was observed for larger doses. These maximum areas are about 20% smaller than the extrapolated values determined by the CO-titration method of the previous section. This is partly a result of the base line must lie between the line shown and a horizontal line.

When large exposures of oxygen were used, either high p_{O_2} or large dose time, the background shifted further upward and it became more difficult to distinguish the background and the decay curve. Furthermore the background level, as defined in Fig. 7, decayed less rapidly after a large oxygen dose. These data suggest that part of the area between the background curves of Fig. 7 and the base line reached after a lengthy evacuation period is attributable to CO_2 arising when CO reacts with oxygen diffusing to the surface from the bulk. The uptake of oxygen by Pd substrates has been reported previously (*17*) and is presently being investigated in more detail. The important point is that significant amounts of oxygen can be incorporated into Pd and at least some part of it may become available for CO_2 production during and after the surface oxygen is depleted.

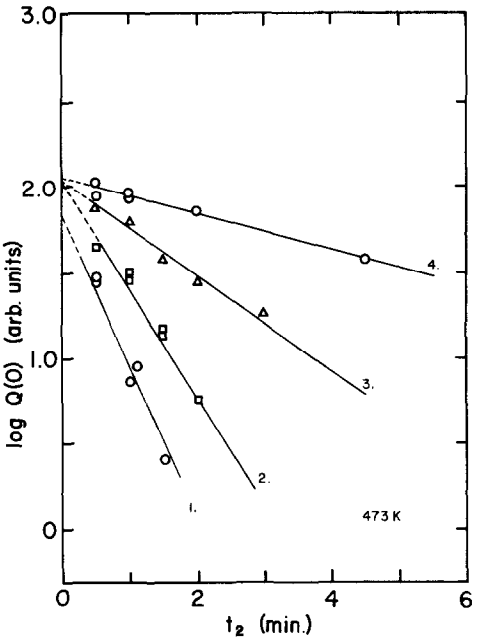

FIG. 8. The variation of O(a) at 473 K, as determined from the area of peak A, with evacuation time t_2 for a variety of oxygen doses. Prior to O_2 dosage, $p_{CO} = 4.0 \times 10^{-6}$ Pa. The dose pressure of O_2 was 8.0×10^{-6} Pa and for each curve the dose and exposure time are: (1) 2.4×10^{-4} Pa · s, 30 s; (2) 4.8×10^{-4} Pa · s, 60 s; (3) 1.4×10^{-3} Pa · s, 180 s; (4) 7.2×10^{-3} Pa · s, 900 s.

Figure 8 shows in a systematic way how the area of peak A varies with evacuation time t_2. This data and that of Fig. 6 show clearly that $Q_0(O)$ is independent of oxygen dosage except when the dose is very light. There is however a systematic decrease in the slope as the oxygen dosage increases. This can be understood in terms of surface and nonsurface oxygen assuming that during heavy dosage some oxygen penetrates the bulk palladium and slowly becomes available for CO_2 production during t_2. Since $Q_0(O)$ is independent of oxygen dose under our conditions, the method of determining the area of peak A includes only the surface oxygen present at the end of period t_2. The latter depends on oxygen dosage through the participa-

tion of nonsurface oxygen but cannot exceed the saturation coverage present at $t_2 = 0$. This model supposes that nonsurface oxygen is partially depleted after the initial preparatory phase and prior to the oxygen dose.

We now have two methods for determining oxygen coverage under working conditions—(1) titration of O(a) by CO(g) and extrapolation as in Figs. 6 and 8 and (2) analysis of CO_2 decay following termination of oxygen dosage. The former is useful when the CO pressure is low during t_2, because the decrease of O(a) is relatively slow and it is possible to titrate using a large pressure of CO and then extrapolate to find Q_0(O). If during t_2 the CO pressure is relatively high, then O(a) decreases rapidly and this method can not be applied practically. On the other hand, the latter method is powerful when the CO pressure during t_2 is high but it cannot be applied when CO is low because there is only a small decline in the CO_2 pressure when the oxygen dose is terminated and it is difficult to fix the base line CO_2 pressure. In any case, analysis of the decay of CO_2 pressure curves is subject to considerable systematic error as discussed above.

SUMMARY

The reaction path of the carbon monoxide oxidation has been studied on a polycrystalline palladium substrate prepared by heavy exposure to oxygen at high temperatures. Transient phenomena were monitored after CO dosing with preadsorbed oxygen and vice versa. Two different reaction paths were found to prevail. (1) An Eley–Rideal path, $CO(g) + O(a) \rightarrow CO_2(g)$, prevails when preadsorbed oxygen is dosed with CO. (2) A Langmuir–Hinshelwood path, $CO(a) + O(a) \rightarrow CO_2(g)$, is important when preadsorbed CO is dosed with oxygen.

The former reaction can be used to titrate adsorbed oxygen under working conditions and two methods can be used determine the adsorbed oxygen. The first is useful when CO pressure under working conditions is low while the latter is useful when the working CO pressure is high.

ACKNOWLEDGMENTS

The authors thank J. S. Close, D. B. Almy, and D. C. Foyt for assistance with the apparatus and for many stimulating conversations regarding this research. We also thank Virginia Hale and Donna Jackson for invaluable assistance in preparing the manuscript.

REFERENCES

1. Baddour, R. F., Modell, M., and Hausser, U. K., *J. Phys. Chem.* **72,** 3621 (1968).
2. Baddour, R. F., Modell, M., and Goldsmith, R. H., *J. Phys. Chem.* **74,** 1987 (1970).
3. Tracy, J. C., and Palmberg, P. W., *J. Chem. Phys.* **51,** 4852 (1969).
4. Horgan, A. M., and King, D. A., *Trans. Faraday Soc.* **67,** 2145 (1971).
5. Weinberg, W. H., *J. Catal.* **29,** 173 (1973).
6. Yao, Y. F. Y., and Kummer, J. T., *J. Catal.* **28,** 124 (1973).
7. Soma-Noto, Y., and Sachtler, W. M., *J. Catal.* **32,** 315 (1974).
8. Bonzel, H. P., and Ku, R., *J. Vac. Sci. Technol.* **9,** 663 (1971).
9. Bonzel, H. P., and Ku, R., *Surface Sci.* **33,** 91 (1972).
10. Bonzel, H. P., and Ku, R., *J. Chem. Phys.* **59,** 1641 (1973).
11. Winterbottom, W. L., *Surface Sci.*, **36,** 705 (1973).
12. Ertl, G., and Rau, P., *Surface Sci.* **15,** 443 (1969).
13. Ertl, G., and Koch, J., *Z. Phys. Chem. N. F.* **69,** 323 (1970).
14. Ertyl, G., and Koch, J., *in "Adsorption–Desorption Phenomena"* (F. Ricca, Ed.), p. 345. Academic Press, New York, 1972.
15. Ertl, G., and Koch, J., *Proc. Int. Congr. Catal. 5th, 1972* p. 969 1973.
16. Ertl, G., and Neumann, M., *Z. Phys. Chem. N. F.* **90,** 127 (1974).
17. Close, J., and White, J. M., *J. Catal.* **36,** 185 (1975).
18. Matsushima, T., Almy, D. B., Foyt, D. C., Close, J. S., and White, J. M., *J. Catal.* **39,** 277 (1975).
19. Tamaru, K., *in* "Advances in Catalysis" (D. D. Eley, H. Pines and P. B. Weisz, Eds.), Vol. 15, p. 65. Academic Press, New York, 1959.
20. Matsushima, T., and White, J. M., unpublished data.